

# A NEW STRIPLINE KICKER FOR PF-AR TRANSVERSE FEEDBACK DAMPER

R. Takai\*, T. Honda, T. Nogami, T. Obina, Y. Tanimoto, M. Tobiyama

KEK Accelerator Laboratory and SOKENDAI, 1-1 Oho, Tsukuba, Ibaraki 305-0801, Japan

## Abstract

A feedback damper equipped with a long stripline kicker was used to damp transverse beam oscillation at the Photon Factory Advanced Ring (PF-AR), which is a 6.5-GeV synchrotron radiation source of KEK. Recently, the stripline kicker was renewed to one having shorter electrodes and a smaller loss factor because its insulating support was broken by the beam-induced thermal stress and caused frequent electric discharges inducing dust trapping phenomena. In this paper, we present details of the new stripline kicker, from design to installation, as well as demonstrate results of beam oscillation damping obtained with the new kicker.

## INTRODUCTION

The Photon Factory Advanced Ring (PF-AR), which is a 6.5-GeV electron storage ring of KEK, is known as a unique synchrotron radiation source dedicated to single-bunch operations to provide high-intensity pulsed X-rays. It is operated in decay mode in which the stored beam current is added twice daily up to 60 mA. The principal parameters of the PF-AR are listed in Table 1.

Table 1: Principal Parameters of the PF-AR

Operation Energy	6.5 GeV
Injection Energy	2.85 GeV
Stored Current	60 mA
RF Frequency	508.57 MHz
Circumference	377.26 m
Harmonic Number	640
Number of Bunches	1
Revolution Frequency	795 kHz
Tunes (x/y/s)	10.17/10.23/0.05
Damping Time (x/y/s)	2.5/2.5/1.2 ms
Natural Emittance	294 nm rad
Natural Bunch Length	18.6 mm (62 ps)

A long stripline feedback kicker comprising four stainless steel pipes with length of about 1.4 m was installed in the west straight section of the ring to damp the transverse oscillations of injected and stored beams. In order to reduce their self-weight deflection, an insulating support made of machinable ceramics “Photoveel [1]” was attached at the midpoint of each electrode. Since user operation commenced in the autumn of 2012, we frequently observed sudden increases in the vacuum pressure accompanied by beam loss around these insulating supports. Inspection of the kicker enabled us to find the damaged insulating supports. We considered this damage to have

been caused by thermal stress due to energy loss of the stored single bunch. These supports were previously suspected to cause frequent electric discharges, thereby inducing dust trapping phenomena [2]. Photos of the original kicker electrodes and their insulating support parts taken during the inspection are shown in Fig. 1. Although the time domain reflectometry (TDR) response was acceptable, we found that the head of the bolt supporting the kicker electrode via the Photoveel part discolored to become black due to electric discharges and the Photoveel part itself was partially melted and broken. We continued the user operation by reducing the maximum stored current from 60 mA to 55 mA so as not to exceed the threshold of electric discharges because it was difficult to repair the damaged insulating supports in a short time. A new stripline kicker was designed and fabricated in parallel with this restricted user operation, and finally installed in the summer of 2015.

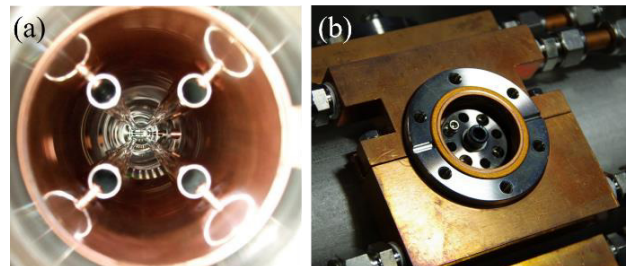


Figure 1: Photos of (a) the original kicker electrodes and (b) their insulating support parts.

In this paper, we describe the details of our new stripline kicker, from design to installation, and show the results of beam oscillation damping with the new kicker.

## DESIGN OF STRIPLINE KICKER

### Shunt Impedance

To quantitatively evaluate the stripline kicker performance, we need to calculate the transverse shunt impedance defined as follows [3]:

$$R_{\perp} = \frac{V_{\perp}^2}{2P}, \quad (1)$$

where  $P$  is the rms input power to the kicker electrode, and  $V_{\perp}$  is the transverse deflecting voltage generating between the electrodes. This deflecting voltage for a vertical kick is calculated using the following expression:

$$V_{\perp} = \left| \int_0^L [E_y(z) + cB_x(z)] dz \right|, \quad (2)$$

\* ryota.takai@kek.jp

where the beam propagates in the  $z$ -direction,  $c$  is the speed of light,  $L$  is the length of the kicker electrode, and  $E_y(z)$  and  $B_x(z)$  are the vertical electric and horizontal magnetic fields, respectively. Note that we took no account of the beam transient effect because the deflecting fields experienced by the propagating beam in the kicker are almost constant in our case. The deflecting fields for arbitrary kicker structures were numerically calculated by the HFSS simulation code [4]. The validity of the numerical calculation was verified in advance assuming a simple stripline kicker whose shunt impedance can be calculated analytically.

### Design Policies

At first, the original kicker was modeled and its transverse shunt impedance was calculated by the above numerical method to define our design policies. As shown in Fig. 1, the original kicker is composed of four stainless steel pipes rotated by  $45^\circ$  from the orthogonal symmetric position. The outer diameter and length of the each electrode are 18 mm and 1360 mm, respectively. These are mounted in a 101.3-mm-inner-diameter beam duct so that the center of the each electrode is positioned 36 mm apart from the center of the duct. The characteristic impedance of each electrode is approximately  $54 \Omega$ . Supposing a case when we use it as a vertical kicker and input a high-frequency power of 1 W at 20 MHz<sup>1</sup> from the four downstream ports with the dipole mode, then the transverse shunt impedance was calculated to be 193 k $\Omega$  by Eqs. (1) and (2). Since we were able to sufficiently suppress the beam oscillation with the original kicker, we set the following equation as a necessary condition to be satisfied by the new kicker:

$$R_{\perp} > 190 \text{ k}\Omega @ 20 \text{ MHz} . \quad (3)$$

We need not be overly concerned about the electrode length, namely the kicker bandwidth, because the PF-AR is dedicated to single-bunch operation.

Besides, it is important to minimize the energy lost when the beam passes through the kicker structure (a loss factor) to suppress the heat generation of the kicker electrode, which may cause machine troubles. In the numerical simulation with GdfidL [5], the loss factor of the original kicker was estimated to be 250 mV/pC for an electron beam with a bunch length of 8.3 mm (28 ps). When converted into the power loss for the beam current of 60 mA, it becomes 1.1 kW. Since this power loss increases to 1.5 kW when there is an insulating support at the midpoint of each electrode, we can see that about 400 W of power had been lost around the support. In addition to condition (3), the new kicker is also required to satisfy the following condition:

$$P_{\text{loss}} < 1.1 \text{ kW} @ 60 \text{ mA} . \quad (4)$$

<sup>1</sup> This frequency almost corresponds to the upper limit of the bandwidth of our final power amplifiers.

### Basic Structure

Based on these design policies, three basic structures were considered for the new kicker: Types A, B, and C. Cross-sectional shapes at the input/output port position of the three structures are shown in Fig. 2. In Type A, the original pipe electrodes are replaced with concaved electrodes shaped like a cylinder divided into four sections in the longitudinal direction. The inner diameter of the circular beam duct was set to 90 mm according to the inner horizontal width of racetrack-shaped ducts connected to both ends of the kicker. The electrode thickness is 2 mm and the electrode width was chosen such that the opening angle relative to the duct axis becomes  $60^\circ$ . The distance from the duct axis to the electrode surface was determined to be 33.9 mm by using HFSS such that the characteristic impedance of each electrode becomes 50  $\Omega$ . The shunt impedance calculation showed that 1380-mm-long electrodes are required to satisfy condition (3) in this structure ( $R_{\perp} = 198 \text{ k}\Omega @ 20 \text{ MHz}$ ). The loss factor for the beam of the same bunch length as the original kicker simulation was estimated to be 134 mV/pC, corresponding to a power loss of 600 W. That is, the power loss is reduced by half, but electrodes of the same length are required to generate the same deflecting voltage compared to the original kicker.

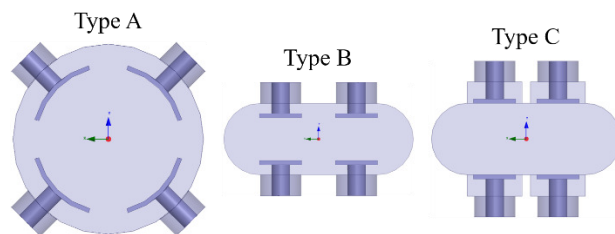


Figure 2: Basic structures considered for the new stripline kicker.

As mentioned above, the normal beam duct of the PF-AR is racetrack-shaped with inner horizontal and vertical widths of 90 mm and 34 mm, respectively. In Type B, the planar electrodes are built directly in the normal duct. In such a structure, there is no need to install additional shape-conversion ducts that cause the power loss. Since the internal space is restricted, two sets of parallel planar electrodes, with thickness of 2 mm and width of 20 mm, are arranged in the horizontal direction. The closest horizontal and vertical distances between the electrodes are set to 16 mm and 20.4 mm, respectively. In this structure, the transverse shunt impedance in the horizontal direction is different from that in the vertical direction because of the asymmetric pattern of the electrodes. Considering that the vertical shunt impedance is smaller than the horizontal one, 900-mm-long electrodes are sufficient to clear condition (3) ( $R_{\perp v} = 229 \text{ k}\Omega @ 20 \text{ MHz}$ ). The loss factor was estimated to be 164 mV/pC, corresponding to a power loss of 740 W. Although the vertical aperture of this structure is narrow, it has good deflecting efficiency and a smaller power loss than the original kicker.

Type C has a structure in which the same planar electrodes as Type B are contained in recess grooves provided

in the top and bottom faces of the normal duct. The closest horizontal distance between the electrodes was narrowed to 10 mm because of 3-mm gaps provided between the groove and the electrode. Since the electrodes are arranged to be flush with the inner duct surface, the closest vertical distance between the electrodes is 34 mm. The groove depth was set to be 10.2 mm such that the characteristic impedance of each electrode becomes  $50 \Omega$ . The electrode length required to comply with condition (3) was calculated to be 1200 mm ( $R_{\perp v} = 199 \text{ k}\Omega @ 20 \text{ MHz}$ ). The loss factor was estimated to be 104 mV/pC, corresponding to a power loss of 470 W. As planned, the power loss significantly decreased, but the electrode cannot be shortened that much to attain the required length. Furthermore, in case such a cavity-like structure is provided, we have to devise a structure to avoid trapping a part of the higher-order modes of the beam wakefield in the structure; for example, smoothing the step difference sections at both ends of each groove to suppress the beam wakefield.

We evaluated the basic structure of the new kicker from the above three candidates and decided to adopt Type B, which has the shortest electrodes and requires no shape-conversion ducts. However, in order to avoid the characteristic impedance mismatch due to the self-weight deflection without insulating supports that cause additional power losses, the 900-mm-long electrodes should be divided into two 450-mm-long electrodes arranged in the longitudinal direction.

### Minor Improvement

When actually fabricating the Type-B structure, we added a minor improvement. To improve the mechanical strength of each electrode, the width was extended outward by 5 mm, and each extending section was bent inward with an angle of  $45^\circ$ . The characteristic impedance of each electrode was readjusted to be  $50 \Omega$  by narrowing the vertical distance between the electrodes to 17.6 mm (the closest vertical distance is 10.5 mm). According to this improvement, almost the same shunt impedance as before the improvement could be obtained even by the 860-mm-long electrodes ( $R_{\perp v} = 247 \text{ k}\Omega @ 20 \text{ MHz}$ )<sup>2</sup>. The loss factor slightly increased to 200 mV/pC, corresponding to a power loss of 900 W, but it remains smaller than that of the original kicker. Although the total power loss may increase if the long electrodes are divided in half along the longitudinal direction, it is not expected to become a serious problem because there are no lossy structures such as insulating supports. Figure 3 shows the longitudinal beam coupling impedance for the improved kicker evaluated by the GdfidL simulation. Relatively large peaks around 4 GHz are considered not to be trapped locally because the cut-off frequency of the normal duct is 1.8 GHz.

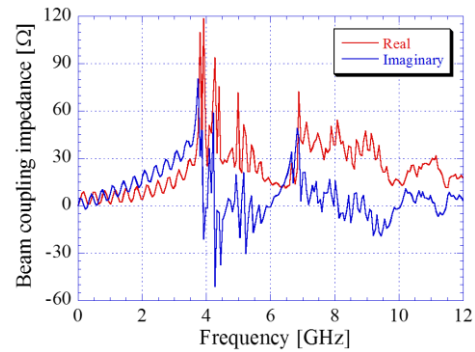


Figure 3: Real and imaginary parts of the longitudinal beam coupling impedance for the improved kicker. The simulated beam bunch length is 8.3 mm (28 ps).

## FABRICATION AND INSTALLATION

Two of the same kicker ducts were fabricated corresponding to the divided electrodes. The electrode length of each kicker duct was extended to 460 mm so that the ceramics seals of feedthroughs located at both ends of each electrode cannot be directly seen from the beam. The beam coupling impedance will not be affected by this change. A schematic drawing of one of the two kicker ducts and a photo of the internal electrodes are shown in Fig. 4. The kicker duct and electrodes were produced from a stainless steel. The inner surface of the duct, and the surface of the electrodes were coated with copper to reduce the beam-induced wall heating. Furthermore, a special feedthrough with a bending structure on the inner conductor was used as one of the two feedthroughs supporting each electrode to absorb the longitudinal thermal elongation [6]. Physical interference between the adjacent feedthrough flanges (EIA-7/8) was prevented by changing the inner conductor length. The characteristic impedance of each electrode was measured by TDR and adjusted to be in the range of  $50 \pm 2 \Omega$  by using 0.2-mm-thick shim rings.

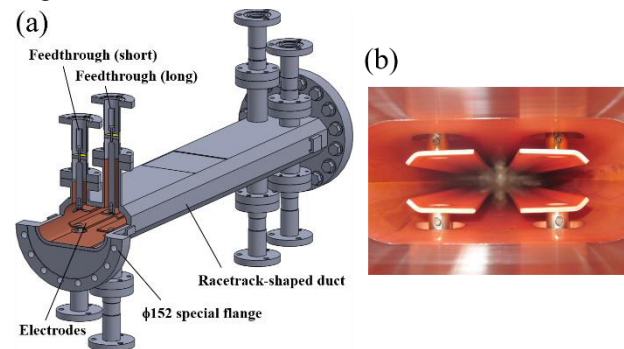


Figure 4: (a) Schematic drawing of the new stripline kicker duct and (b) photo of the inner electrodes.

The two kicker ducts were arranged in series and installed in the southwest straight section of the ring. For the time being, we use them as a long kicker by connecting the adjacent ports with each other by short coaxial cables. They can also be used as two broadband kickers in future. Figure 5 shows a photo of the installed kicker

<sup>2</sup> As for the horizontal direction, the shunt impedance was calculated to be 485 k $\Omega$ , which is sufficient to satisfy condition (3).

ducts and a block diagram of the PF-AR feedback damper system including the new kicker. The beam signal is picked up by dedicated striplines and inputted to the analog detection circuit named “Bunch Oscillation Detector (BOD) [7]” via a low pass filter, programmable attenuator, and gating module. The horizontal and vertical oscillation components detected by the BOD are combined with each other after phase control and pulse modulation, after which they are sent to the final broadband amplifiers (R&K, A20-200-R). The amplified feedback signals are fed to the new kicker from the four downstream ports and kick back the oscillating beam. The output signals from the four upstream ports are attenuated by 20-dB dummy loads and sent to the local control room for monitoring. Each port of the kicker and each dummy load are cooled by airflow and their temperatures are constantly monitored by operators.

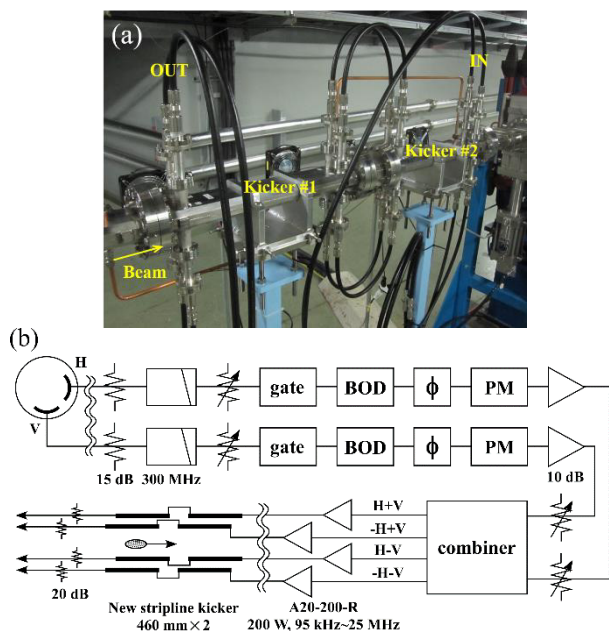


Figure 5: (a) Photo of the installed kicker ducts and (b) block diagram of the PF-AR feedback damper system. PM in the block diagram stands for pulse modulator.

We demonstrated that the new kicker functions correctly by performing a damping test of the beam oscillation excited by the tune measurement system. At the PF-AR, betatron tunes are measured by superposing the tracking generator output of a spectrum analyzer (Advantest, U3741) for monitoring the BOD output on the feedback kicker input. We excited betatron oscillations by using this system and checked whether the amplitudes of the tune spectra were changed, depending on the opening/closing of the feedback loop. The results for the horizontal and vertical directions are shown in Fig. 6. These spectra were obtained by averaging over 10 independent measurements with a stored beam current of 42 mA. On closing the feedback loop, we can see that the spectral amplitudes decrease by approximately 11 dB and 5 dB for the horizontal and vertical directions, respectively. In addition, we have also confirmed that spectral peaks due to beam instabilities, which appear only in the horizontal

direction spontaneously, disappear when the feedback loop is closed. These results demonstrate that the new kicker works correctly as a part of the feedback damper system.

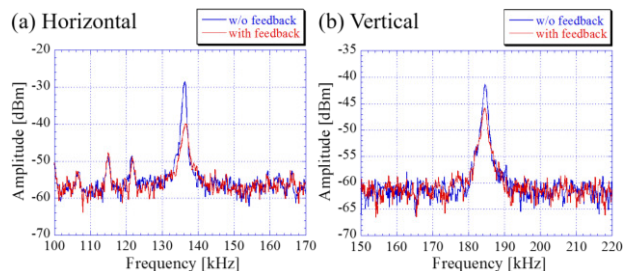


Figure 6: Tune spectra for the (a) horizontal and (b) vertical directions excited by the tune measurement system. The origins of a few peaks on the lower-frequency side of the horizontal tune are unknown.

## SUMMARY AND FUTURE PLANS

The stripline kicker for the PF-AR feedback damper system was renewed. The new kicker can realize a higher shunt impedance and a smaller power loss with shorter electrodes compared to those achieved with the original kicker. The new kicker was installed in the southwest straight section of the ring in the summer of 2015, and exhibits good damping performance for beam oscillation. Abnormal signs such as sudden increases in the vacuum pressure and rapid heat generations of the kicker components have not been observed since the installation.

A new beam transport line for the PF-AR (AR-BT) enabling the 6.5-GeV full-energy injection is under construction since July 2016. Beam commissioning using the new AR-BT will start in January 2017. The dedicated striplines to detect beam oscillation at the front end of the damping system will be replaced with an existing button BPM not used for COD correction during commissioning. The feasibility of this replacement has already been confirmed with the actual stored beam. In the near future, we plan to renew the aging analog circuits including the BOD as well.

## REFERENCES

- [1] <http://www.ft-ceramics.co.jp/eng/products/machinable/Mica/>
- [2] Y. Tanimoto, T. Honda, and S. Sakanaka, “Experimental demonstration and visual observation of dust trapping in an electron storage ring”, *Phys. Rev. ST Accel. Beams*, vol. 12, p. 110702, 2009.
- [3] D. A. Goldberg and G. R. Lambertson, “Dynamic Devices: A Primer on Pickups and Kickers”, *AIP Conf. Proc.*, vol. 249, p. 537, 1992.
- [4] <http://www.ansys.com/Products/Electronics/ANSYS-HFSS>
- [5] <http://www.gdfidl.de/>
- [6] M. Arinaga *et al.*, “Progress in KEKB beam instrumentation systems”, *Prog. Theor. Exp. Phys.*, vol. 2013, p. 03A007, 2013.
- [7] P. L. Pellegrin, “T.A.R. Bunch Oscillation Detector”, TRISTAN Design Note, TN-82-011, 1982.